This article was downloaded by:
On: *25 January 2011*
Access details: *Access Details: Free Access*
Publisher *Taylor & Francis*
Informa Ltd Registered in England and Wales Registered Number: 1072954 Registered office: Mortimer House, 37-41 Mortimer Street, London W1T 3JH, UK

Liquid Crystals

Publication details, including instructions for authors and subscription information:
http://www.informaworld.com/smpp/title~content=t713926090

Electrohydrodynamic instability in a binary mixture of cyanobiphenyls in a d.c. field

R. K. Medya; R. N. P. Choudhary; P. K. Mahapatra

Online publication date: 06 August 2010

To cite this Article Medya, R. K. , Choudhary, R. N. P. and Mahapatra, P. K.(1999) 'Electrohydrodynamic instability in a binary mixture of cyanobiphenyls in a d.c. field', Liquid Crystals, 26: 6, 795 — 807

To link to this Article: DOI: 10.1080/026782999204480

URL: http://dx.doi.org/10.1080/026782999204480

PLEASE SCROLL DOWN FOR ARTICLE

Full terms and conditions of use: http://www.informaworld.com/terms-and-conditions-of-access.pdf

This article may be used for research, teaching and private study purposes. Any substantial or systematic reproduction, re-distribution, re-selling, loan or sub-licensing, systematic supply or distribution in any form to anyone is expressly forbidden.

The publisher does not give any warranty express or implied or make any representation that the contents will be complete or accurate or up to date. The accuracy of any instructions, formulae and drug doses should be independently verified with primary sources. The publisher shall not be liable for any loss, actions, claims, proceedings, demand or costs or damages whatsoever or howsoever caused arising directly or indirectly in connection with or arising out of the use of this material.

LIQUID CRYSTALS, 1999, VOL. 26, NO. 6, 795–807

Electrohydrodynamic instability in a binary mixture of cyanobiphenyls in a d.c. field

R. K. MEDYA, R. N. P. CHOUDHARY*
Department of Physics and Meteorology, Indian Institute of Technology,
Kharagpur-721 302, India

and P. K. MAHAPATRA
Department of Physics, Vidyasagar University, Midnapore, West Bengal, India

(*Received in final form 5 November 1998; accepted 7 November 1998*)

Electrohydrodynamic instability in a homeotropically oriented liquid crystal mixture, with positive dielectric anisotropy, has been studied under a d.c. electric field. Various studies on textures at different voltage were also made. The existence of charge injection, charge diffusion and convective flow of liquid in the liquid crystal cells was found. The effect of viscosity, dielectric anisotropy and other physical parameters on electric current through the sample cells, is discussed. A small change in phase transition temperature on application of an electric field was found in the thin cell of the sample material.

1. Introduction

The occurrence of electrohydrodynamic (EHD) instability in isotropic liquids is due to the interaction of the applied electric field with the charge injected from the electrodes in the liquid. It is analogous to thermally induced Rayleigh–Benard instability [1, 2] and is known as the Felici instability (FI) [3]. A nematic liquid crystal also experiences this type of instability and, because of the peculiar anisotropic properties of the LC the instability is made visible [2]. Williams and Hellmeir [4–6] observed domain patterns of homogeneously aligned nematic liquid crystals with negative dielectric anisotropy in d.c. and a.c. electric fields. The occurrence of the instability in the above system was successfully explained by the Carr–Helfrich instability (CHI) [7, 8]. This type of instability occurs exclusively in liquid crystals with negative or zero dielectric anisotropy [2]. In liquid crystals of the (+, +) and (−, −) classes [first symbol gives the sign of dielectric anisotropy ($\varepsilon_{\parallel} - \varepsilon_{\perp}$); second symbol gives the sign of ($\sigma_{\parallel} - \sigma_{\perp}$), conductivity anisotropy], it was not expected to see any instability because of the presence of strong electric and elastic torques, which have a tendency to stabilize the liquid crystal structure [9]. But Nakagawa and Akahana [10] studied the liquid crystal 5CB, with (+, +) anisotropy and observed cellular domains in a homeotropically oriented sample. The observed instability was explained by the Felici-type instability and is named 'Felici–Benard' instability (FBI). Later Rout and Chaudhary [11, 12] observed this FBI in liquid crystals with positive dielectric anisotropy [8CB and 8OCB]. Transient current flow phenomenan in 5CB, 8CB and 8OCB were also studied and a very slow relaxation ($\sim 10^2$ s) was observed indicating the existence of a charge diffusion process [10–12]. It seems that the role of dielectric and conductivity anisotropy of the EHD instability in a nematic liquid crystal is still not clear. Further, as the anisotropy in physical properties of nematic liquid crystals has a great influence on fluid flow, the EHD instability could also be influenced by the said anisotropy.

The device parameters and physical properties of pure materials can be enhanced or changed drastically by mixing two or more compounds in various ratios. From the preliminary physical data on mixtures of two or more cyanobiphenyls [13] it is clear that some of these mixtures have very interesting properties and may be very useful for devices.

In view of the importance of mixed liquid crystals we have taken for study a mixture S_1 which is a eutectic two cyanobiphenyls and has a small nematic range. With this limited nematic range, the values of various physical parameters may be changed considerably with rise in temperature, and the effect of these changes on

---

*Author for correspondence.

Journal of Liquid Crystals ISSN 0267-8292 print/ISSN 1366-5855 online ©1999 Taylor & Francis Ltd
http://www.tandf.co.uk/JNLS/lct.htm
http://www.taylorandfrancis.com/JNLS/lct.htm

textures and EHD instability in a d.c. electric field can be easily observed. The usefulness of the material in device applications can also be studied.

2. Experimental

To study the LC mixture, cells were prepared as follows. Antimony doped SnO_2 coated glass plates, prepared by us, were used as electrodes, and sample films were sandwiched between pairs of electrodes. The separation between two electrodes was pre-determined by using Mylar spacers; spacers of four different thickness were used. Using a diamond cutter, the effective area of the electrodes was made $64\,mm^2$ for each cell. The SnO_2 coated glass plates were treated with CTAB (cetyl trimethyl ammonium bromide) to ensure homeotropic alignment of the LC molecules. The temperature was controlled and measured with a Mettler central processor (FP-80) and hot stage (FP-82); the accuracy of temperature measurement was 0.1°C. The hot stage was mounted on a polarizing microscope for visual observations and microphotography. A d.c. voltage was applied to the LC cells with the help of dry cells and a potentiometer; current flowing through the cells was measured by a digital picoammeter (Scientific Equipment, Model DPA-111). An electric circuit was developed by us to measure the current through four cells simultaneously. A thin film of arbitrary thickness of the liquid crystal, between PVA-treated thin glass slides, was prepared and textures were studied at different temperatures. The rate of change of temperature during texture studies was held at $0.2°C\,min^{-1}$. The diffusion process in the liquid crystal was studied by the transient current technique; Switching transients were recorded for a d.c. step voltage of 2 V switched on and off across the sample cell. Data recording was performed with a digital 'memoryscope' (Iwatsu DMS-6430) with a data length of 1024 WD.

3. Results

3.1. *Microscopic studies*

The texture studies of the sample showed the following phase transition sequence:

$$\mathrm{SmA} \overset{43°C}{\longleftrightarrow} \mathrm{N} \overset{45°C}{\longleftrightarrow} \mathrm{I}$$

(SmA = smectic A phase, N = nematic phase, I = isotropic phase.) Slightly higher phase transition temperatures were found than reported previously [13].

Figures 1 (*a*)–(*i*) show the gradual appearance of domains with the increase of applied d.c. voltage to the sample cell of thickness 50 μm at 44.3°C. All the micrographs were taken under crossed analyzer and polarizer conditions. When the applied voltage was zero, there was no texture, i.e. dark texture were observed, however some bright spots were seen in some cells, due to improper alignment of the LC molecules. For small applied voltage (< 2.5 V), there was no change in the texture; above this voltage, the scattered bright spot textures vanished and dark view over all the cell was observed.

With further increase of applied voltage, cellular type domains started appearing [figure 1 (*a*)]. The minimum voltage required for the appearance of domain pattern, referred as the threshold voltage (V_{th}) for EHD instability was 3.7 V at 44.3°C for a 50 μm thick cell. With the other cells, V_{th} was found to be 3.65, 3.5 and 3.5 V for the 17, 23 and 75 μm thick cells, respectively. It was seen that with the increase of $(T - T_{Sm-N})$ V_{th} decreased (T_{Sm-N} is the SmA↔N transition temperature and T is the temperature of the sample): for the 50 μm cell, values of V_{th} were 3.6 and 3.4 V at 44.7°C and 45°C respectively. It was interesting to observe that during the nematic–isotropic transition the minimum voltage required for domain formation was higher.

With further increase of applied voltage, cellular domains began to elongate and finally formed a well organized roll-like pattern distributed throughout the cell area. At 6 V, disorder in the domain patterns began and became complete at 7 V; convective flow in the liquid crystal became rapid above 8 V. At this point the movement of dust particles was clearly seen. At any temperature very close to T_{Sm-N} the shape of the rolls were seen to be irregular and slightly distorted; V_{th} values were high (figures 2 (*a*) and 2 (*b*) for a 75 μm cell at 44.3°C], but with further increase of temperature, the rolls appeared regular and spread over the cell [figures 2 (*c*) and 2 (*d*) for a 75 μm cell at 45°C].

For thinner cells (17 and 23 μm), the roll-like textures had smaller roll widths (figures 3 (*a*)–(*c*) and 4 (*a*), (*b*)]. This observation confirms the assumption that the vortex diameter of the vertical flow of liquid in the cell is approximately equal to the cell thickness [2]. It was also observed that at higher applied electric field, the liquid crystal suffered chemical dissociation, and some empty areas developed within the thin cells [figure 4 (*b*) for a 17 μm cell]. We were therefore unable to make observations for higher electric fields.

3.2. *Electrical measurements*

3.2.1. *Current–voltage characteristics*

Figures 5 (*a*)–(*d*) show the variation of current (I) with voltage (V) at different temperatures in the four different cells. When the voltage was below 2 V, a very small current flowed; this was due to ohmic conduction of

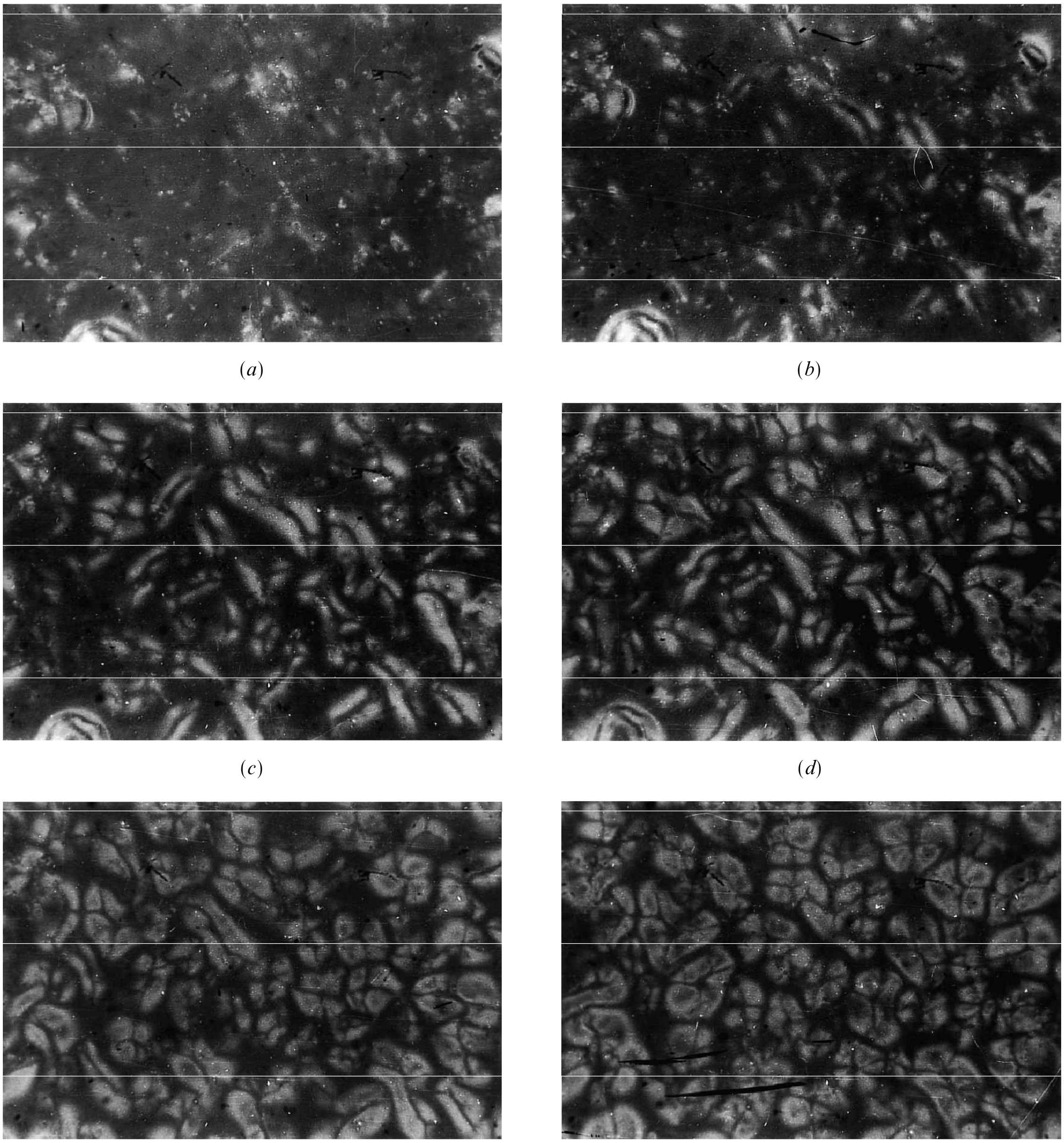
(*a*) (*b*)

(*c*) (*d*)

(*e*) (*f*)

Figure 1. Microphotographs of domain patterns in a sample of S_1 (magnification 150×) for the 50 μm thick cell with applied voltage (*a*) 3.7 V, (*b*) 4.0 V, (*c*) 4.5 V, (*d*) 5.0 V, (*e*) 5.5 V, (*f*) 6.0 V, (*g*) 6.5 V, (*h*) 7.0 V, (*i*) 8.0 V, at 44.3°C.

current through the liquid crystal. In both the smectic and nematic phases, with increasing applied voltage (> 2 V), the current increased at a higher rate.

In the SmA phase, the current was found to be very small. In the thicker cells, the current started to increase at 2 V; above 3.5 V the rate of increase in current dropped significantly. In thinner cells, above 4.5 V the current stopped increasing. In the smectic phase, no convective flow of liquid was observed up to 10 V.

It has been shown experimentally [14] that in a liquid crystal under a d.c. electric field, charge injection becomes significant in explaining an instability such as FBI [5, 6]. One can now conclude that above 2 V, charge injection takes place and a diffusion current starts to flow in addition to the ohmic part, but no component flows due to fluid convection. As the current is injection dependent it tends to attain a constant value for thicker cells above 3.5 V. However, in thinner cells (at 42°C), it

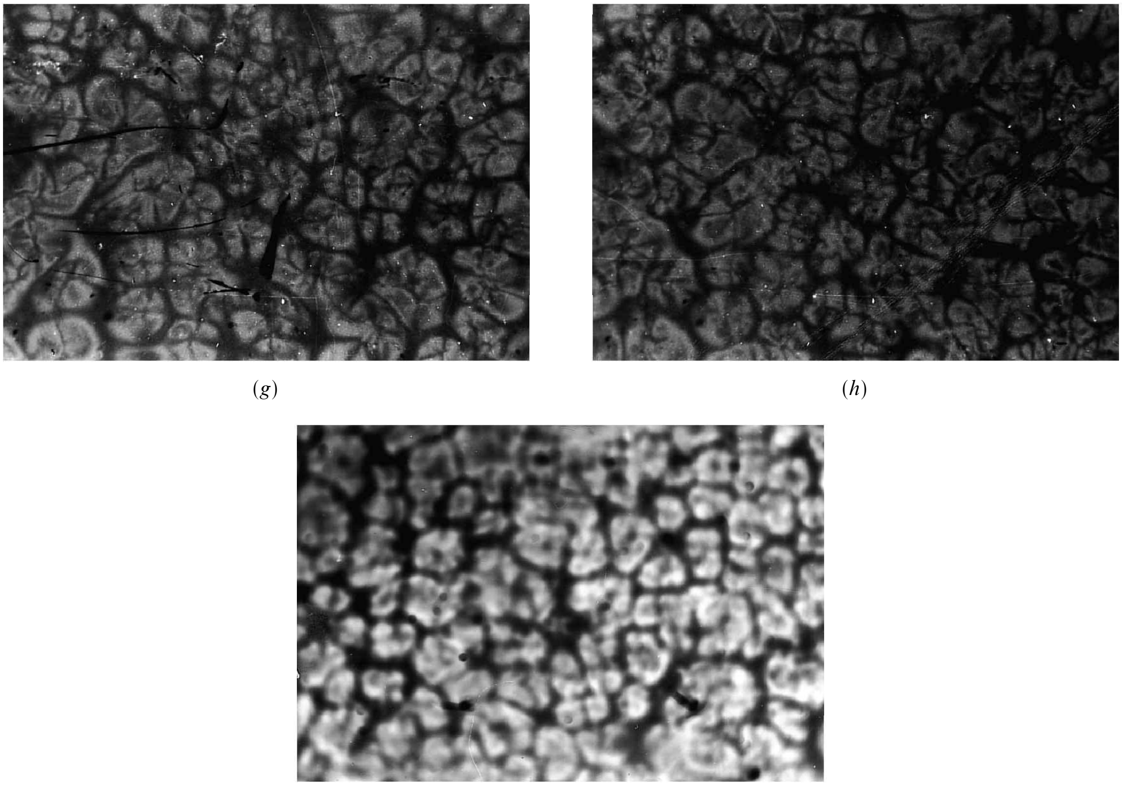

(g) (h)

(i)

Figure 1. (continued).

increases continuously (with a slower rate) with increase of applied voltage. Applied electric field in thinner cells was found to be higher than that in thick cells, causing higher charge diffusion at temperatures close to the smectic–nematic phase transition.

In thick cells in the nematic phase, above 3 V applied voltage the current was found to increase rapidly; for the isotropic liquid state it started to increase above 2.5 V. In thinner cells it began to increase just above 2 V. A similar form of $(I-V)$ characteristics for 8CB and 8OCB was observed in their nematic phase by Rout and Choudhary [11, 12]. Above V_{th}, the force exerted on the space charge was sufficient to start convection flow in the liquid crystal, and then cellular domains appeared; Charge transfer with liquid flow was induced. As the voltage increases above V_{th}, the current due to charge transfer with convective flow of liquid becomes dominant and the total current increases rapidly with voltage. When the liquid crystal was in the isotropic phase, similar $(I-V)$ characteristics were observed, however the current was higher.

3.2.2. *Current–temperature characteristics*

Figures 6 (a)–(d) show the $(I-T)$ characteristics at different applied voltages. A sharp increase in conductivity occurred at a temperature close to SmA–N phase transition for 17 μm and 23 μm cells [within 42.5–43.5°C] and for 50 μm and 75 μm cells [within 43.5–44°C]. In the nematic and isotropic phases conductivity increases with increase in temperature, but at a lower rate. The $(I-T)$ characteristics for 8CB & 8OCB have an exponential nature [11, 12], but in the mixture sample these characteristics were different. Above $T_{\mathrm{Sm-N}}$, the current was found to increase rapidly up to 44°C and then slowly with increasing temperature.

It has been shown experimentally that in nematic LC cells, under a d.c. field, charge injection from the electrodes plays the major role in EHD instability [14, 15]. Nakagawa and Akahana [10] and Rout and Choudhary [11, 12] used the following Richardson's emission law to explain the EHD instability in liquid crystals 5CB, 8CB and 8OCB.

$$J = AT^2 \exp(-\Phi/kT) \tag{1}$$

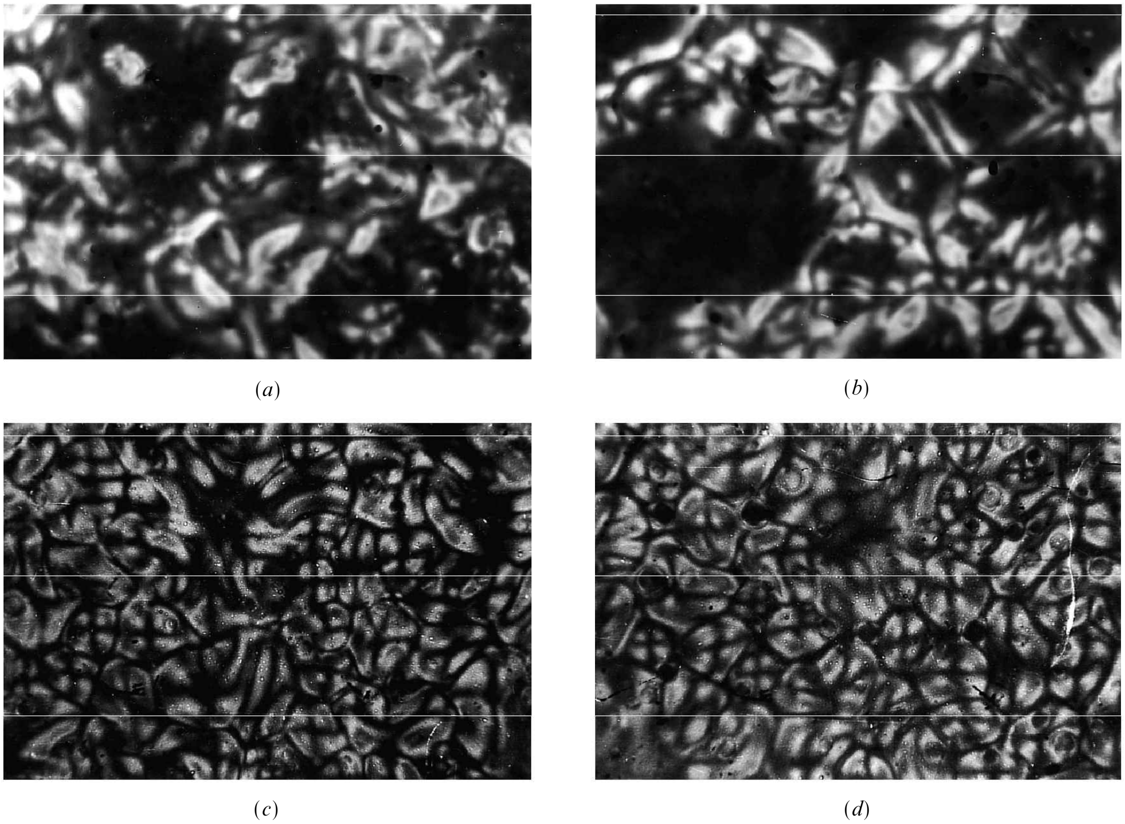

Figure 2. Photomicrographs of domain patterns in S_1 (magnification 150×) for the 75 μm thick cell with applied voltage (*a*) 4.0 V, (*b*) 5.0 V at 44.3°C; and (*c*) 4.0 V, (*d*) 5.0 V at 45.0°C.

where T = absolute temperature of the cell, k = Boltzmann constant, A = a constant and Φ = the thermionic work function. Both A and Φ depend on electrode materials, surface condition and applied electric field. To examine the applicability of equation (1) to the sample under study, $\ln(I/T^2)$ vs $(10^3/T)$ was plotted. For the 75 μm cell [figure 7 (*d*)], the discontinuity at the SmA–N phase transition was found very sharp. For 50 μm cells, it was also sharp [figure 7 (*c*)] but for the other two cells the sharpness in discontinuity was not prominent. From the slope of the graphs plotted, the work function Φ of SnO_2 coated electrodes was calculated and values were found within 0.6–1.1 eV. Although the previous workers [10–12] found a definite relation between applied voltage and Φ, we could not find such a relationship, thus equation (1) was not useful for the liquid crystal mixture S_1.

3.2.3. *Existence of the diffusion process*

Nakagawa observed the existence of a slow relaxation process; Rout explained it as a result of the charge diffusion process in the LC cell. Chang *et al.* [16] also showed that the decay time T_d is inversely proportional to the diffusion constant D and directly proportional to the square of the sample thickness L

$$T_d = L^2/\pi^2 D. \qquad (2)$$

Rout conducted transient current experiments and showed the validity of the empirical relation

$$I(t \propto (D/t)^{1/2} \qquad (3)$$

where $I(t)$ = current at time t after switching off the supply voltage. The results of our transient current experiment have been plotted in figure (8) as $I(t)$ vs t transient traces. Values taken from that figure, $I(t)$ vs $t^{-1/2}$ are plotted in figures 9 (*a*)–(*d*). This shows that equation (3) holds good for $t \geq 1.3$, 1.5, 1.6 and 1.9 s for 17, 23, 50 and 75 μm thick cells, respectively.

4. Discussion

The current density J in an isotropic liquid as well as in a nematic liquid crystal (under EHD instability), contains three main terms [3] and can be written as

$$J = \sigma E + J_{\mathrm{diff}} + J_{\mathrm{conv}} \qquad (4)$$

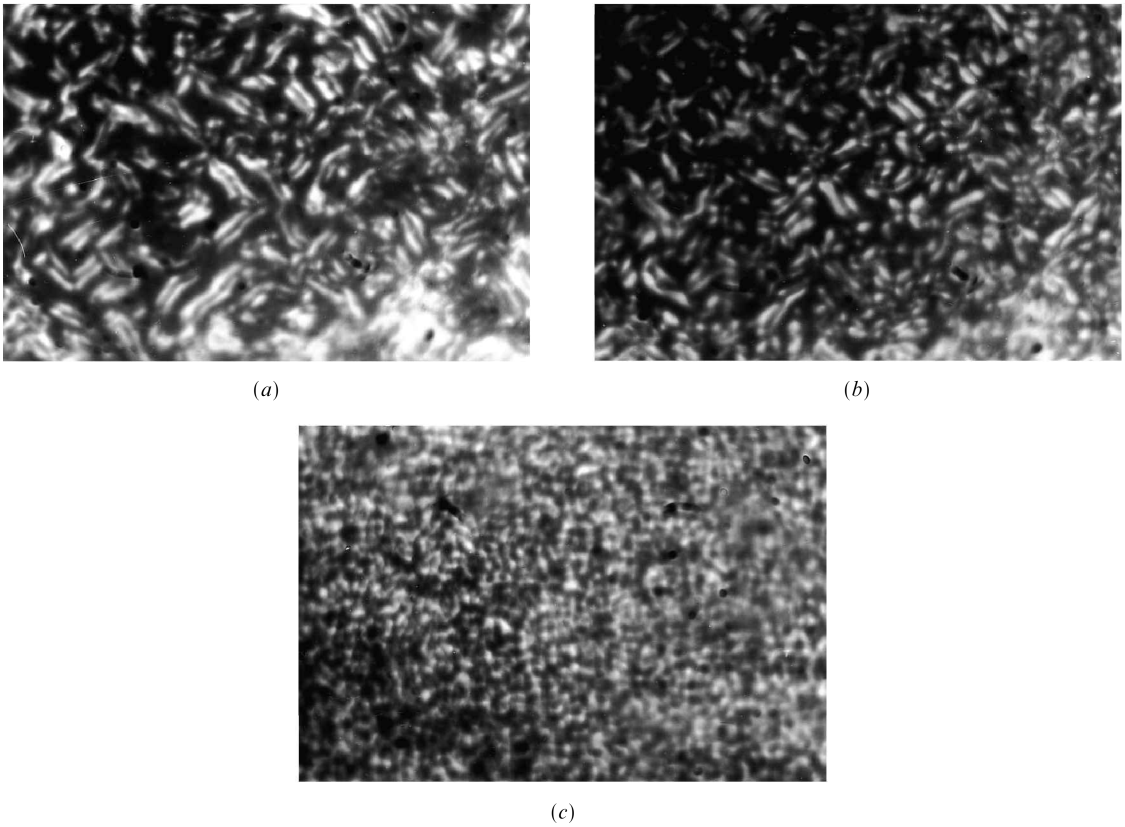
(a) (b) (c)

Figure 3. Photomicrographs of domain patterns in S_1 (magnification 150×) for the 23 μm thick cell with applied voltage (a) 4.0 V, (b) 4.5 V, (c) 6.0 V at 44.0°C.

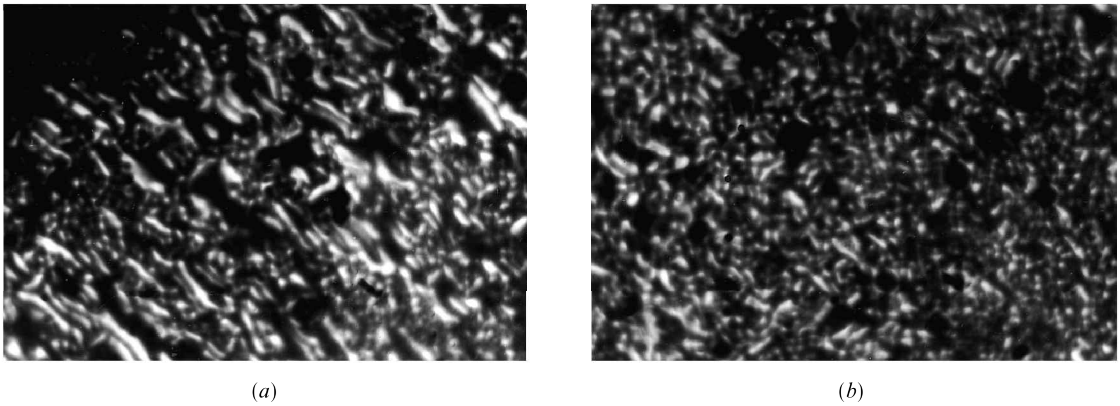
(a) (b)

Figure 4. Photomicrographs of domain patterns in S_1 (magnification 150×) for the 17 μm thick cell with applied voltage (a) 5.5 V, (b) 7.0 V at 43.8°C.

where σE is an ohmic term (σ= electrical conductivity, E= applied electric field), J_{diff} is a diffusion term resulting from the charge concentration gradient and J_{conv} is a convection term due to charge transfer in the moving liquid.

Our microscopic observations and electrical results can be explained using this equation as follows:

(i) For an applied voltage of less than 2 V, a very small current flows which may be due to ohmic conduction.

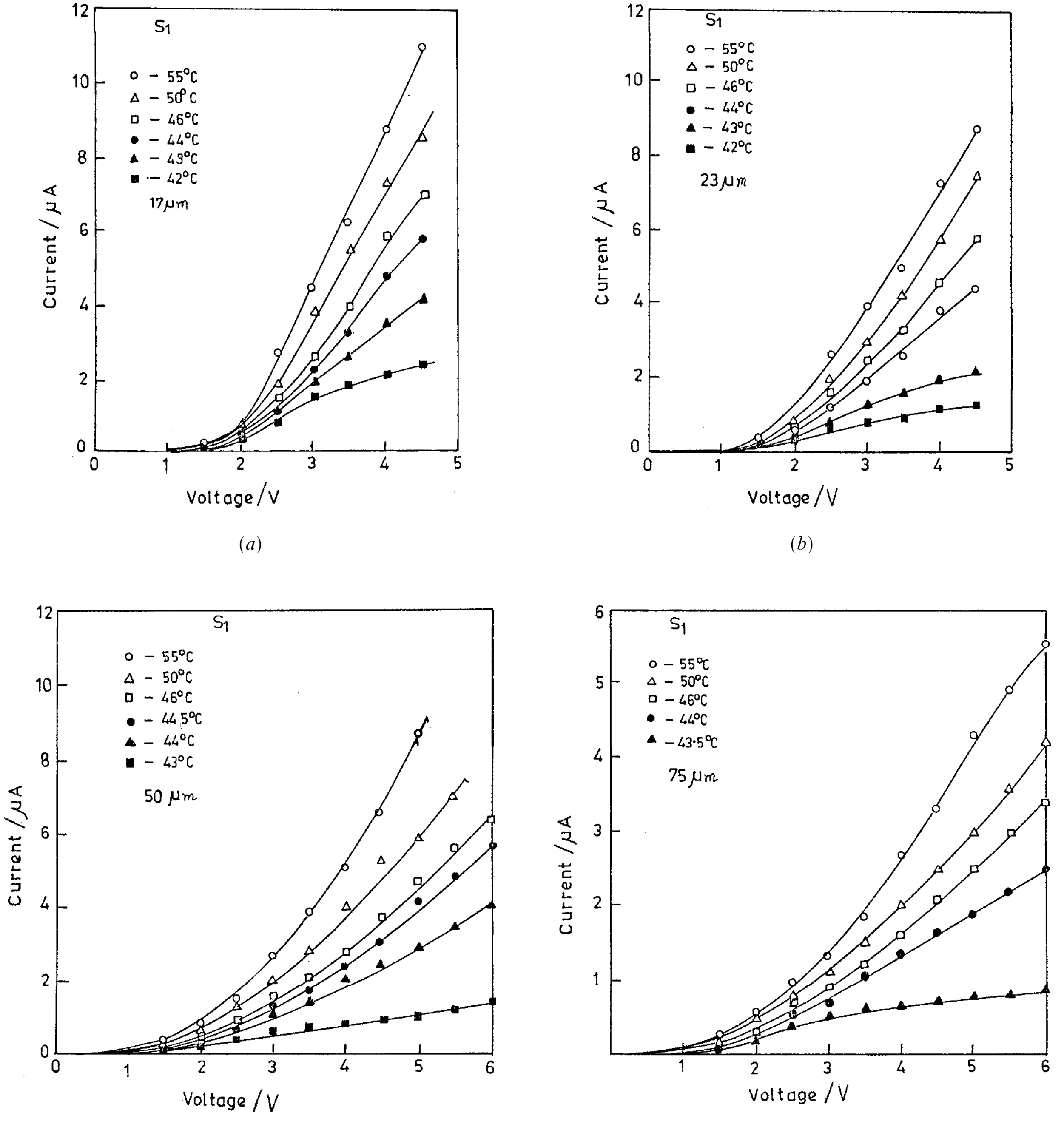

(a) (b)

(c) (d)

Figure 5. Current–voltage characteristics at different temperatures for S_1 for cell thickness (a) 17 μm, (b) 23 μm, (c) 50 μm, (d) 75 μm.

(ii) For $2\,V <$ applied voltage $< V_{th}$, the conductivity increases gradually with applied voltage. It may be due to charge injection from the cathode since antimony doped SnO_2 is an n-type semiconductor. This increases negative charge in the vicinity of the cathode and a charge diffusion current starts to flow; the total current then grows more rapidly.

(iii) For $V > V_{th}$ convective flow in the liquid starts, EHD instability appears and an abrupt increase in electric current is found; at this time J_{conv} becomes dominant. Further increase in the external electric field increases the convective flow of liquid and the electric current grows rapidly. The increase in fluid flow with applied field is clearly observed in microscopic observations.

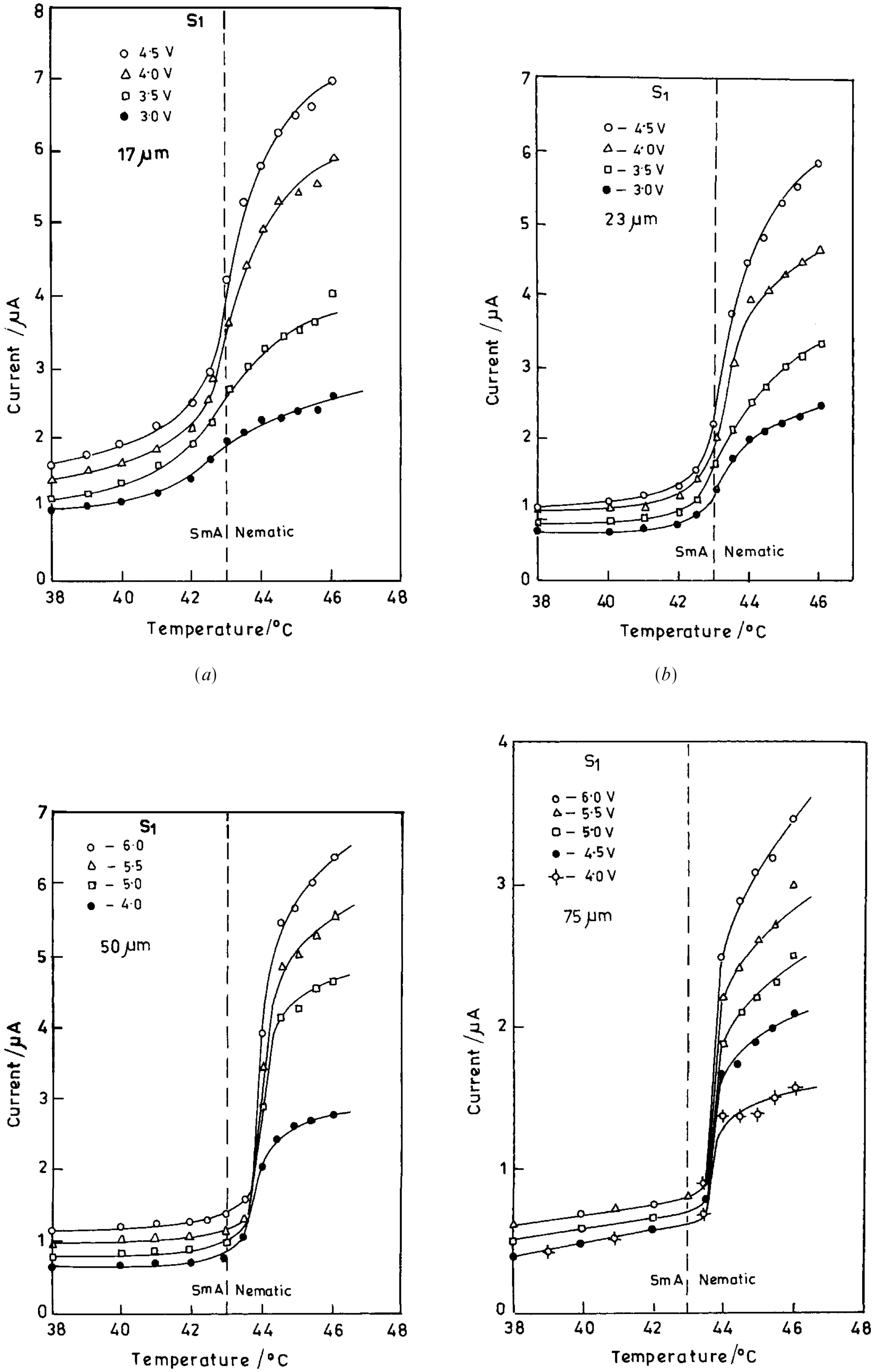

(*a*) (*b*)

(*c*) (*d*)

Figure 6. Current–temperature characteristics at different voltages for S_1 for cell thickness (*a*) 17 μm, (*b*) 23 μm, (*c*) 50 μm, (*d*) 75 μm.

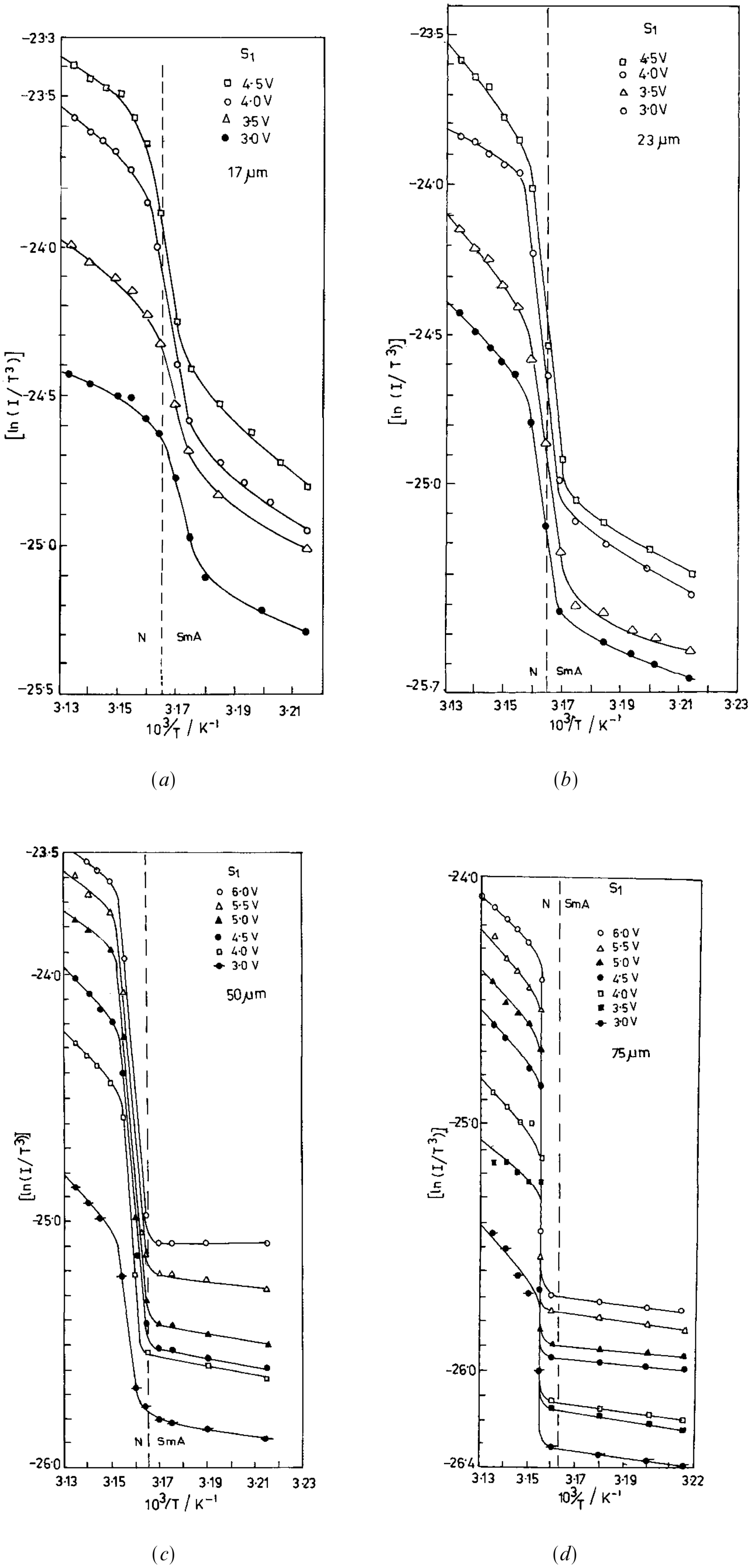

(a)

(b)

(c)

(d)

Figure 7. The plots of ln(I/T^2) against $10^3/T$ at various applied voltages for S₁ for cell thickness (a) 17 μm, (b) 23 μm, (c) 50 μm, (d) 75 μm.

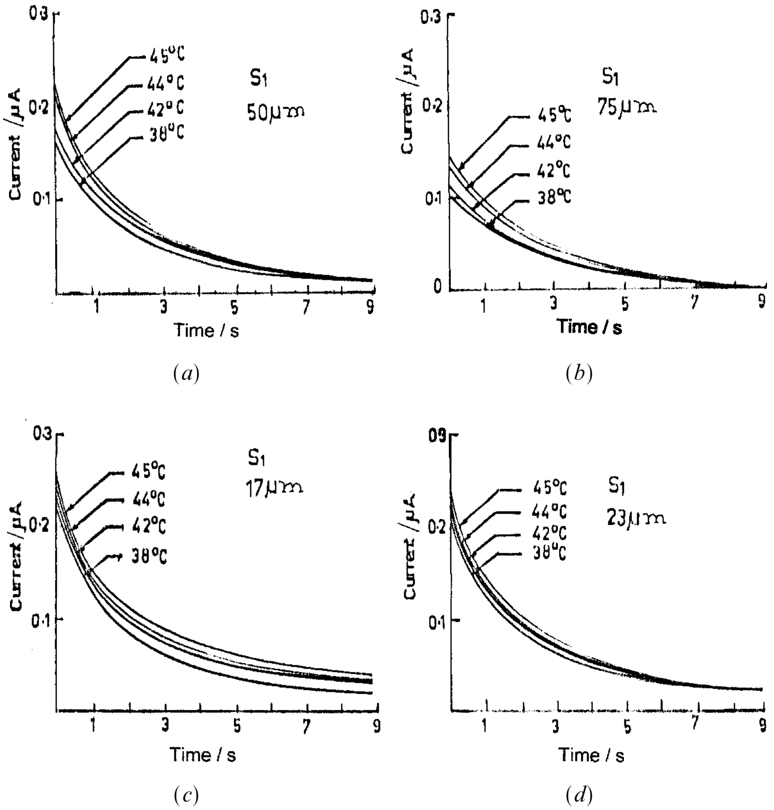

(*a*) (*b*)

(*c*) (*d*)

Figure 8. The transient current for S_I at different temperatures for cell thickness (*a*) 50 μm, (*b*) 75 μm, (*c*) 17 μm, (*d*) 23 μm.

In the optical studies, some bright spots were found due to improper alignment in some cells, although above 2.5–3 V, there textures vanished and the view became dark over all the cell. The voltage required to complete this type of transition was found to decrease with increasing temperature. It was also observed that in the SmA phase the required voltage was rather high and that after the SmA–N phase transition, it dropped significantly.

In liquid crystals of positive dielectric anisotropy ($\Delta\varepsilon > 0$), Fréedericksz transition from planar to homeotropic alignment is possible if an electric field is applied along the cell thickness. The threshold voltage for this transition depends on the splay elastic constant and dielectric anisotropy [$V_{\text{thf}} = C\ (K_{11}/\Delta\varepsilon)^{1/2}$, where V_{thf} = threshold voltage for the Fréedericksz transition, C = constant, K_{11} = splay elastic constant] [17].

The material (S_I) can be used in optical switching devices with a small operating d.c. voltage (2–3 V), over a small temperature range (43–45°C). Keeping the applied voltage above the V_{thf}, and if the material is cooled, the homeotropic alignment remains unchanged after the N to SmA phase transition. Hence S_I can be used in optical memory devices at room temperature (smectic range of S_I is 0–43°C).

The appearance of darkness in the texture is due to the completion of homeotropic alignment of its molecules by the external field plus the internal field created by inhomogeneous charge distribution in the LC cells. From these observations it is clear that this liquid crystal mixture has positive dielectric anisotropy; its splay elastic constant is temperature dependent and higher in the smectic phase than in the nematic phase.

From theoretical considerations [2], it has been shown that the threshold voltage required to initiate EHD instability is

$$V_{\text{th}} = k\eta\mu/\varepsilon \tag{5}$$

where k = constant, η = viscosity coefficient, ε = dielectric permittivity and μ = ionic mobility. V_{th} is thus thickness independent. In our experiments V_{th} was found to be approximately same for all four cells. A small difference in V_{th} may be due to non-identical surface conditions of different cells, and a slight decrease in V_{th} with increase in temperature was found. In figures 6(*a*)–(*d*), current values were found to remain nearly unchanged at and above 44°C at 3 V which indicates that ionic mobility, μ, does not significantly change with temperature in the nematic phase. The temperature dependence of dielectric

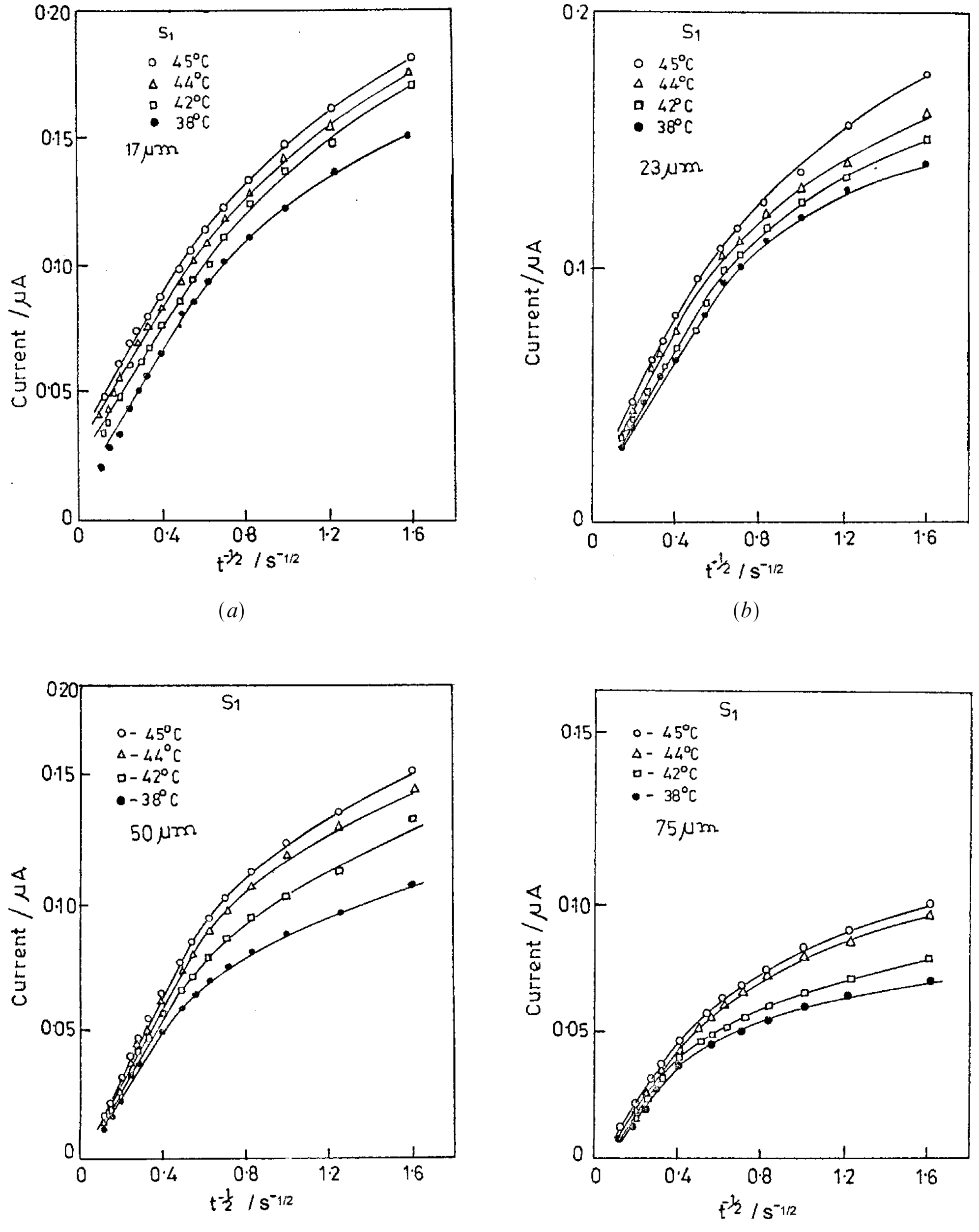

(*a*) (*b*)

(*c*) (*d*)

Figure 9. (*a*) Plots of $I(t)$ against $t^{-1/2}$ for S1 for cell thickness (*a*) 17 μm, (*b*) 23 μm, (*c*) 50 μm, (*d*) 75 μm.

permittivity, ε, in the nematic phase is also small [18]; within the temperature range, 44–45°C, it can be taken as constant. From the relation (5), therefore, the viscosity of the nematic liquid crystal can be considered to decrease with increasing temperature [19].

At a temperature very close to the N–I transition, the voltage required to develop roll-like domains was found to be higher. This was because, when the temperature difference ($T_{N\text{–}I} - T$) was very close to zero, the order parameter became very small [20]. The thermal vibrations of the directors about their mean direction became faster, and the voltage required to make the optical patterns visible was higher than the actual threshold voltage required to start EHD instability, V_{th}, [21].

In our study of LC material S1, equation (1) was not applicable, especially in the thinner cells. Charge injection from the electrodes was the main reason for EHD instability, but the flow of liquid during this instability determines the current, the $(I-T)$ characteristics of S_1 should therefore be explained in relation to the change in viscosity with temperature. This change in viscosity plays an important role in fluid flow and has a great influence on the convection part, J_{conv}, of the electric current. From figures 6 (*a*)–(*d*) it is clear that just after the SmA–N phase transition, the current changes rapidly with the increase of $(T - T_{\mathrm{Sm-N}})$, up to 44°C. Within the temperature range 43–44°C, the viscosity and elastic properties of the liquid crystal may be reduced significantly with increasing temperature. This condition allows an easier flow of liquid, and a sharp rise in current occurs. Above 44°C, the viscosity may decrease exponentially [19] with rising temperature; the current then increases with rising temperature but at a lower rate.

The temperature sensitivity of the electric current within the temperature range 43–44°C for S_1 is very high and because of this peculiarity, within this temperature range, the mixture can be used in temperature sensors. Changing the mixing ratio of the ingredients, the above temperature range can be adjusted, which is not possible in pure liquid crystals.

In the isotropic phase from the movements of impurities in the liquid, and from the $(I-T)$ characteristics, it is seen that there is little difference in the EHD instability in the nematic and isotropic phases of the mixture S_1.

From microscopic observations, it was found that at temperatures close to $T_{\mathrm{Sm-N}}$, the shape of the domain was irregular and distorted but with increasing temperature it became well organized and roll-shaped [figures 2 (*a*)–(*d*)]. The higher temperature induces an easier deformation in molecular alignment [22]. In addition, at temperatures close to $T_{\mathrm{N-I}}$, the order parameter decreases with increasing temperature [20]. During the motion of the nematic liquid crystal the directors experience a rotating hydrodynamic torque proportional to the velocity gradient (i.e. $M_{\mathrm{hydro}} \propto k.\ \nabla V$, where $V =$ velocity, and k is a friction coefficient with a dimension of viscosity [2]). In the nematic phase, k (like viscosity), is temperature dependent [23] and the fluid flow and the domain shape may be influenced by the reduction of the hydrodynamic torque.

For 17 and 23 μm thick cells, phase transition temperatures were found to decrease slightly with an applied electric field. It was also found that for those cells, conductivity increased at 42.5°C. In thinner cells, an applied voltage created a higher electric field and hence induced a higher electric current. This disturbed the space charge distribution in the cells, perturbing the long range attractive electrostatic forces between the molecules and reducing the SmA–N transition temperature.

5. Conclusion

The LC mixture S_1 shows a planar to homeotropic transition in the nematic phase at a threshold voltage 2.5 V which is very high in the smectic phase. In the nematic phase this voltage is slightly temperature dependent. This threshold voltage depends on the splay elastic constant, which decreases with increasing temperature; in the smectic A phase its value is significantly higher than in the nematic phase.

The current flow in S_1 consists of three terms: (a) an ohmic conduction term, (b) a diffusion term resulting from the gradient of the charge carrier concentration and (c) a convective term due to charge transfer with convective flow of liquid. Convective flow starts above a threshold voltage and EHD instability appears, viscosity consequently plays a major role in fluid flow and in electrical conduction through the sample cell.

In thinner cells of S_1, the phase transition temperature are influenced by the external electric field in these cells, high electric fields induce chemical changes which create empty spaces in the cells and reduce the effective area of the cell.

The LC material S_1 can be used in optical switching devices, temperature sensors, infrared-to-visible image converters and other important applications.

References

[1] Benard, H., 1901, *Ann. Chem. Phys.*, **23,** 62.
[2] Blinov, L. M., 1986, *Sci. Prog.*, **70,** 263.
[3] Felici, N., 1969, *Rev. gen. Elect.*, **78,** 717.
[4] Williams, R., 1963, *J. chem. Phys.*, **39,** 384.
[5] Williams, R., and Heilmeir, G., 1966, *J. chem. Phys.*, **44,** 638.
[6] Williams, R., 1967, *Adv. Chem. Ser.*, **63,** 61.
[7] Carr, E. F., 1967, *Adv. Chem. Ser.*, **63,** 86.
[8] Helfrich, W., 1969, *J. chem. Phys.*, **51,** 4092.
[9] De Gennes, 1974, *The Physics of Liquid Crystals* (Oxford: Clarendon Press), p. 192.
[10] Nakagawa, M., and Akahana, T., 1983, *J. phys. Soc. Jpn.*, **52,** 3773.
[11] Rout, D. K., and Choudhary, R. N. P., 1988, *Mol. Cryst. liq. Cryst.*, **154,** 241.
[12] Rout, D. K., and Choudhary, R. N. P., 1989, *J. Phys. D. appl. Phys.*, **22,** 289.
[13] Herck Ltd. UK, data sheet of liquid crystals.
[14] Grular, H., and Meier, G., 1971, *Mol. Cryst. liq. Cryst.*, **12,** 289.
[15] Penz, P. A., 1971, *Mol. Cryst. liq. Cryst.*, **141,** 15.
[16] Chang, T. S., Green, P. E., and Loebner, E. E., 1974, *Liquid Crystals and Ordered Fluids*, edited by J. F. Johnson and R. S. Porter, Vol. 2, p. 115.
[17] Xie, Y.-Z., and Ou-Yang, Z., 1983, *Commun. theo. Phys., China*, **2,** 1489.

[18] Rout, D. K., 1989, Ph.D. thesis. 1989, IIT, Kharagpur (India).

[19] Patel, J. S., and Goodby, J. W., 1987, *Optical Engineering*, **26,** 373.

[20] Zaboli, M., Kafle, S. R., Saran, D., and Jain, P. C., 1992, *Indian J. Phys*., **66A,** 583.

[21] Blinov, L. M., Barnik, M. I., and Trufanov, A. N., 1982, *Mol. Cryst. liq. Cryst*., **89,** 47.

[22] Hirata, S., and Tako, T., 1982, *J. phys. Soc. Jpn*., **51,** 2371.

[23] Shin-tson, W., 1990, *Optical Materials*, edited by S. Musikant, Vol. 1, p. 143.